

# Chapter 19B. Analysis of Imaging Spectrometer Data for the Dudkash Area of Interest

By Raymond F. Kokaly and Michaela R. Johnson

## Abstract

Imaging spectrometer data collected over the Dudkash area of interest (AOI) in northeastern Afghanistan were analyzed with spectroscopic methods to identify the occurrence of selected materials at the surface. Absorption features in the spectra of HyMap data were compared to a reference library of spectra of known materials. Carbonates and muscovites cover most of the Dudkash AOI. Distinct patterns of kaolinite occur in localized patterns, especially in the center of the AOI. An analysis of HyMap data to detect gypsum found only a few pixels containing this mineral, adjacent to the mapped locations of the bedded gypsum mineral deposit of Shuraw. The known coal deposits in the Dudkash AOI appear to be associated with areas of kaolinite, kaolinite mixed with muscovite/clay/calcite, and calcite mixed with muscovite/illite. This pattern was also observed in preliminary analysis of imaging spectrometer data for the Takhar AOI. The limestone host rock of celestite was detected; however, more detailed studies of the spectral characteristics of the celestite deposit and its host rocks are needed in order to characterize the resource using imaging spectrometer data.

## 19B.1 Introduction

Past studies of geologic data of Afghanistan revealed numerous areas with indications of potential mineral resources of various types (Peters and others, 2007; Abdullah and others, 1977). Several of these areas were selected for follow-on studies using imaging spectroscopy to characterize surface materials. Imaging spectroscopy is an advanced type of remote sensing that is also known as hyperspectral remote sensing. One of those areas selected for follow-on studies is the Dudkash area of interest (AOI) in northeastern Afghanistan, which is approximately 160 km north of Kabul (fig. 19B-1). The area is believed to have the potential for gypsum and celestite. To help assess these potential resources, high-resolution imaging spectrometer data were analyzed to detect the presence of selected minerals that may be indicative of past mineralization processes. This report contains the results of the spectroscopic data analyses and identifies sites within the Dudkash AOI that deserve further investigation, especially detailed geological mapping, lithologic sampling, and geochemical studies.

## 19B.2 Data Collection and Processing

In 2007, imaging spectrometer data were acquired over most of Afghanistan as part of the U.S. Geological Survey (USGS) project "Oil and Gas Resources Assessment of the Katawaz and Helmand Basins." These data were collected to characterize surface materials in support of assessments of resources (coal, water, minerals, and oil and gas) and earthquake hazards in the country (King and others, 2010). Imaging spectrometers measure the reflectance of visible and near-infrared light from the Earth's surface in many narrow channels, producing a reflectance spectrum for each image pixel. These reflectance spectra can be interpreted to identify absorption features that arise from specific chemical transitions and molecular bonds that provide compositional information about surface materials. Imaging spectrometer data can only be used to characterize the upper surface materials and not subsurface composition or structure. However, subsurface processes can be indicated by the distribution of surface materials.

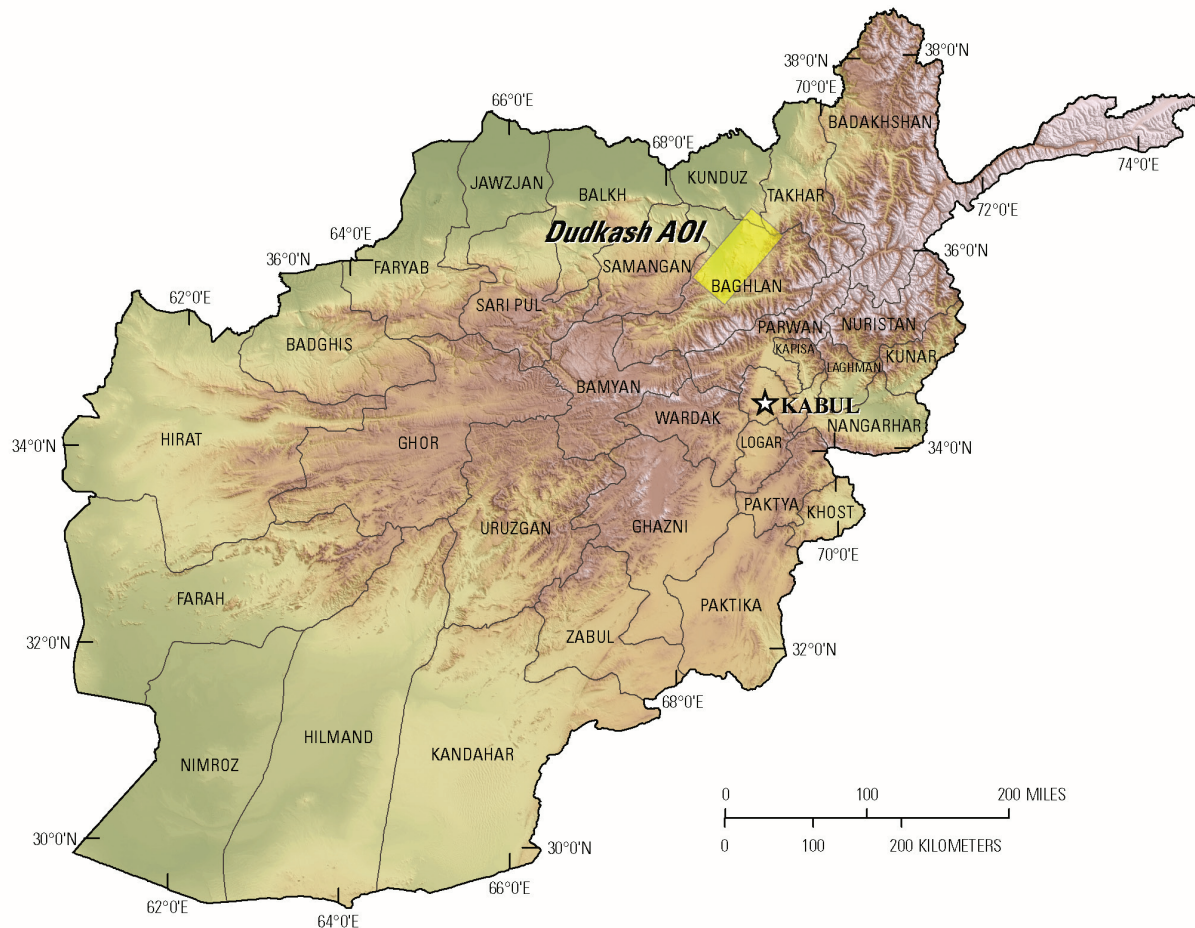


Figure 19B–1. Index map of the Dudkash area of interest in northeastern Afghanistan.

### 19B.2.1 Collection of Imaging Spectrometer Data

The HyMap imaging spectrometer (Cocks and others, 1998) was flown over Afghanistan from August 22 to October 2, 2007 (Kokaly and others, 2008). HyMap has 512 cross-track pixels and covers the wavelength range 0.43 to 2.48 microns ( $\mu\text{m}$ ) in 128 channels. The imaging spectrometer was flown on a WB-57 high-altitude aircraft at approximately 50,000 ft. There were 207 standard data flight lines and 11 cross-cutting calibration lines collected over Afghanistan for a total of 218 flight lines, covering a surface area of 438,012  $\text{km}^2$  (Kokaly and others, 2008). Data were received in scaled radiance (calibrated to National Institute of Standards and Technology reference materials). Before processing, four channels that had low signal-to-noise and (or) were in wavelength regions that overlapped between detectors were removed from the HyMap data. Each flight line was georeferenced to Landsat base imagery in UTM projection (Davis, 2007).

### 19B.2.2 Calibration

HyMap data were converted from radiance to reflectance using a multistep process. This calibration process removed the influence of the solar irradiance function, atmospheric absorptions, and residual instrument artifacts, resulting in reflectance spectra that have spectral features that arise from the material composition of the surface. Because of the extreme topographic relief and restricted access to ground calibration sites, modifications to the typical USGS calibration procedures were required to calibrate the 2007 Afghanistan HyMap dataset (Hoefen and others, 2010). In the first step of the calibration process, the radiance data were converted to apparent surface reflectance using the radiative

transfer correction program Atmospheric CORrection Now (ACORN; ImSpec LLC, Palmdale, Calif.). ACORN was run multiple times for each flight line, using average elevations in 100-m increments, covering the range of minimum to maximum elevation within the flight line. A single atmospherically corrected image was assembled from these elevation-incremented ACORN results. This was done by determining the elevation of each HyMap pixel and selecting the atmospherically corrected pixel from the 100-m increment closest to that elevation.

Each assembled atmospherically corrected image was further empirically adjusted using ground-based reflectance measurements from a ground calibration site. Spectra of five ground calibration sites were collected in Afghanistan: Kandahar Air Field, Bagram Air Base, and Mazar-e-Sharif Airport, as well as soil samples from two fallow fields in Kabul. These were used to calculate empirical correction factors using the pixels of atmospherically corrected HyMap data in the flight lines that passed over the sites. The empirical correction from the closest calibration site to each flight line was applied.

To further improve data quality, an additional calibration step was taken to address the atmospheric differences caused, in part, by the large distances from calibration sites to where the HyMap data were acquired. The large distances were a result of the lack of safe access to ground calibration sites. The duration of the airborne survey and variation in time of day when flight lines were acquired also resulted in differences in atmospheric conditions between standard flight lines and lines over ground calibration sites, which were used to derive the empirical correction factors. During the time of data collection, sun angle, atmospheric water vapor, and atmospheric scattering differed for each flight line. To compensate for this, cross-cutting calibration flight lines over the ground calibration areas were acquired (Kokaly and others, 2008) and used to refine data quality of standard data lines. A multiplier correction for each standard data line, typically oriented north-south, was derived using the pixels of overlap with the well-calibrated cross-cutting line that intersected it, subject to slope, vegetation cover, and other restrictions on pixel selection (Hoefen and others, 2010). As a result, the localized cross-calibration multiplier, derived from the overlap region, corrected residual atmospheric contamination in the imaging spectrometer data that may have been present after the ground calibration step.

### **19B.2.3 Materials Maps and Presentation**

After undergoing a complex and rigorous data calibration process, the georeferenced and calibrated reflectance data were analyzed using the Material Identification and Characterization Algorithm (MICA), a module of the USGS Processing Routines in IDL (Interactive Data Language) for Spectroscopic Measurements (PRISM) software (Kokaly, 2011). The MICA analysis compared the reflectance spectrum of each pixel of HyMap data to entries in a reference spectral library of minerals, vegetation, water, and other materials. The HyMap data were compared to 97 reference spectra of well-characterized mineral and material standards. The best spectral match to each pixel was determined and the results were clustered into classes of materials discussed below. The resulting maps of material distribution, resampled to a  $23 \times 23$  m square pixel grid, were mosaicked to create thematic maps of surface mineral occurrences over the full dataset covering Afghanistan.

MICA was applied to HyMap data twice in order to present the distribution of two categories of minerals that are naturally separated in the wavelength regions of their primary absorption features. MICA was applied using the subset of minerals with absorption features in the visible and near-infrared wavelength region, producing a 1- $\mu\text{m}$  map of iron-bearing minerals and other materials (King and others, 2011), and MICA was applied again using the subset of minerals with absorption features in the shortwave infrared, producing a 2- $\mu\text{m}$  map of carbonates, phyllosilicates, sulfates, altered minerals, and other materials (Kokaly and others, 2011). For clarity of presentation, some individual classes in these two maps were bundled by combining selected mineral types (for example, all montmorillonites or all kaolinites) and representing them with the same color in order to reduce the number of colors required to represent the mineral classes.

The iron-bearing minerals map has 27 identified classes. Iron-bearing minerals with different mineral compositions but similar broad spectral features are difficult to classify as specific mineral species. Thus, generic spectral classes, including several minerals with similar absorption features, such as Fe<sup>3+</sup> type 1 and Fe<sup>3+</sup> type 2, are depicted on the map. The carbonates, phyllosilicates, sulfates, and altered minerals map has 31 identified classes. Minerals with slightly different mineral compositions but comparable spectral features are less easily discriminated; thus, some identified classes consist of several minerals with similar spectra, such as the chlorite or epidote class. When comparisons with reference spectra resulted in no viable match, a designation of “not classified” was assigned to the pixel.

### 19B.3 Geologic Setting of the Dudkash AOI

The Dudkash AOI is mainly within the Baghlan Province in northeast Afghanistan, but the northeast part of it lies within Kunduz and Takhar provinces. The contrast-enhanced stretch of the natural-color composite of Landsat Thematic Mapper bands in figure 19B–2 provides a general overview of the Dudkash AOI terrain and is useful for understanding the general characteristics and distribution of surficial material including rocks and soil, unconsolidated sediments, vegetation, and hydrologic features.

#### 19B.3.1 Topography

Elevations in the Dudkash AOI range between 474 and 4,087 m (fig. 19B–3). The highest areas are in the northeast corner of the Dudkash AOI in sharply defined mountain ranges and foothills that are commonly controlled by faults. The low areas include large agricultural areas in the central and north-central parts of the AOI around the district center of Pul-i-Khumry and the province capitol of Baghlan. Other population centers include the towns of Nahrin in the east and Dushi in the south.

#### 19B.3.2 Lithology and Structure

The oldest rocks in the Dudkash AOI are Middle Proterozoic greenschists, gneiss, quartzite, marble, and amphibolite, exposed in the south-central portion of the area (fig. 19B–4; Abdullah and Chmyriov, 1977; Doebrich and others, 2006). Ordovician sandstones and shales and Silurian–Devonian limestones and dolomites are exposed at the higher elevations along the southeastern edge of the area; however, most of the Dudkash AOI is covered by younger rocks. Lower elevation areas are covered by Paleocene and Late Cretaceous limestones, sandstones, siltstones, and clays, with small occurrences of Eocene rocks of similar type. Lowest elevations are covered by Miocene clays and limestones and Quaternary surficial deposits. Mississippian diorite, granodiorites, and granites and Late Triassic granitic rocks intrude Namurian-stage (Carboniferous), Ordovician, and Silurian–Devonian strata along the southeastern edge of the Dudkash AOI.

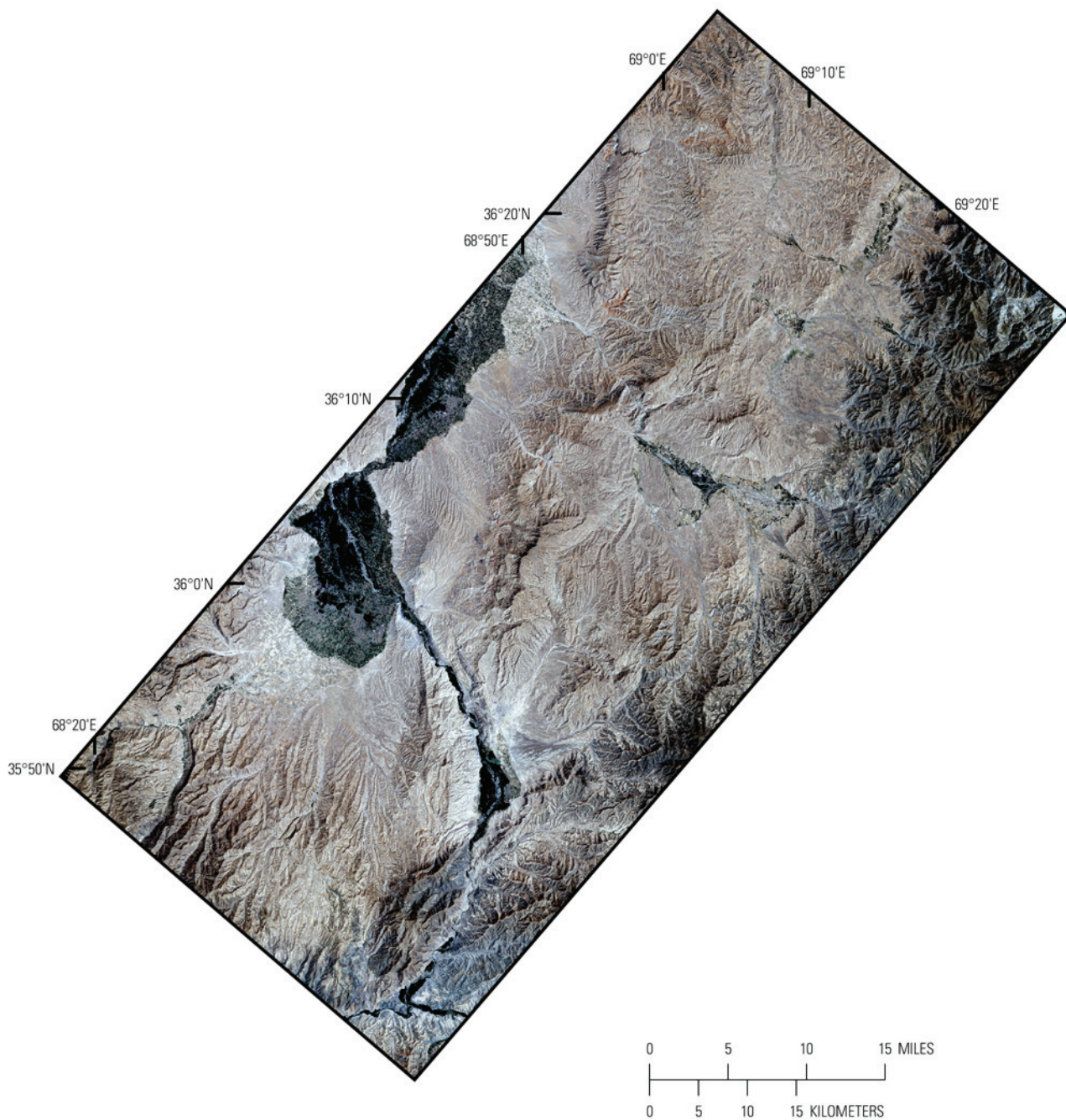
#### 19B.3.3 Known Mineralization

Figure 19B–5 shows 12 locations where mineralization with a potential for mineral resource development may exist (Peters and others, 2007). A number of different types of mineral deposits, particularly strontium-bearing celestite and gypsum deposits are present within the Dudkash AOI. The mineralogical characteristics of the mineralized locations are summarized in table 19B–1. Clay and limestone resources and showings of copper (Cu) and zinc (Zn) are also indicated as occurring in the AOI.

Celestite in the Tangi-Murch deposit is hosted in bituminous limestone. Paleogene carbonate rocks crop out in the area (Abdullah and others, 1977). Beds as much as 170 m long with thicknesses from 0.4 to 1.67 m are indicated (Abdullah and others, 1977).

Bedded gypsum (Dudkash Gypsum) has been found in beds as much as 6 m thick with extensions as much as 12 km in an Upper Jurassic sequence (Abdullah and others, 1977). Gypsum beds at the Shuraw mineral occurrence are 1 m thick and occur in Jurassic sandstone and clay (Abdullah and others, 1977).

Paleocene limestone beds at the Pul-i-Khumry mineral occurrence have been exploited for raw material for a nearby cement plant. The rock is light-colored, thick-bedded, fine-crystalline and found in beds 300 to 400 m thick exposed over an area of several thousand square kilometers (Abdullah and others, 1977).



**Figure 19B–2.** Contrast-enhanced Landsat Thematic Mapper natural-color image of the Dudkash area of interest.

#### **19B.4 Mineral Maps of the Dudkash Area of Interest**

Analysis of the HyMap imaging spectrometer data of the Dudkash AOI using spectroscopic methods resulted in the identification of a wide variety of minerals exposed at the surface. Although the occurrence of certain minerals may suggest that mineralization processes may have once operated in the area, many of the minerals that were identified are also common rock-forming minerals or minerals that

can be derived from the weathering of a wide variety of rock types. Consequently, the distribution patterns of the identified minerals and the geologic context in which they occur are extremely important in understanding the causes of mapped mineral occurrences and evaluating the possible potential for related mineral deposits.

Figure 19B–6 depicts the results of the MICA analyses of the HyMap data for the Dudkash AOI for the 2- $\mu$ m wavelength materials, which include clays, carbonates, phyllosilicates, sulfates, altered minerals and other materials. Figure 19B–7 shows the results for the iron-bearing minerals. The carbonates cover most of the Dudkash AOI, mostly indicated by pixels containing calcite and calcite mixed with clay/mica. However, pixels matched to pure muscovite spectra occur over large contiguous areas both within mapped boundaries of intrusive units but also outside the boundaries and in other areas. Distinct patterns of kaolinite clays occur in localized patterns, especially in the center of the AOI. Epidote and chlorite were found in spatially consistent patterns in the northeast and were especially concentrated near the southern corner of the AOI (see fig. 19B–6). Strong gypsum signatures were only found in three pixels in the 2- $\mu$ m material mapping.

Because of the large number of classes represented and the subtleties of the distribution patterns represented in these image maps, it is instructive to display these results as a series of image maps each depicting a selected group of minerals that are mineralogically related or commonly occur together in special geologic environments (figs. 19B–8 to 19B–12). Figure 19B–8 shows the distribution of carbonate minerals in the Dudkash AOI, whereas figure 19B–9 shows where clay minerals and micas occur. The distribution of iron oxide and hydroxide minerals are displayed in figure 19B–10. Minerals commonly found in hydrothermally altered rocks are mapped in figure 19B–11 and secondary minerals often associated with mineralized and (or) weathered rocks are mapped in figure 19B–12.

#### **19B.4.1 Carbonate Minerals**

Carbonate minerals, either calcite or dolomite, were mapped over a large majority of the Dudkash AOI (fig. 19B–8). In general, calcite is mapped within every geologic unit. Dolomite mixed with calcite and (or) clay occurs in a less spatially extensive pattern, but does occur in localized concentrations and in linear patterns 4 to 8 km in length. None of the known mineralized areas are highlighted by the carbonate minerals map. Because of the ubiquitous nature of carbonate, the Pul-i-Khumry area of limestone mineralization is not uniquely identified, but does occur within a large area of pixels mapped as matching the strong absorption features of abundant calcite. The Dudkash Stone mineral occurrence is found in an area of concentrations of pixels that were matched to dolomite + calcite and clay, consistent with the expected dolomite mineralogy for this fluxstone. The Dudkash Lime mineral deposit is found in an area of pixels that mapped as kaolinite + calcite, calcite + clay, and calcite, consistent with the description of the deposit as limestone beds that crop out between Jurassic clays and siltstones (Abdullah and others, 1977).

#### **19B.4.2 Clays and Micas**

Abundant muscovites were detected in the mapped units of Mississippian and Late Triassic intrusive rocks near the town of Dushi in the southwest part of the Dudkash AOI (fig. 19B–9). In addition, muscovites were also found distributed within nearby Silurian and Jurassic stratified rock units, suggesting that mineral distributions detected with HyMap data could help in the refinement of lithologic contacts. Muscovite was found with strong spectral signatures and spatially coherent patterns in association with Namurian stage stratified rock units. Kaolinites were distributed mostly in Lower to Middle Jurassic units both in the central area of the AOI and near the town of Nahrin, with additional occurrences of spatially consistent groups of pixels in adjacent Early Cretaceous and Late Jurassic units, similar in distribution to the kaolinites in the Takhar AOI (Kokaly and Johnson, chap. 26, this volume). The occurrences of Kaukpar bentonite and Surkhab clay are not near any large areas of mapped montmorillonite, although the pixels around the indicated locations contain a mixture of carbonates and clays.

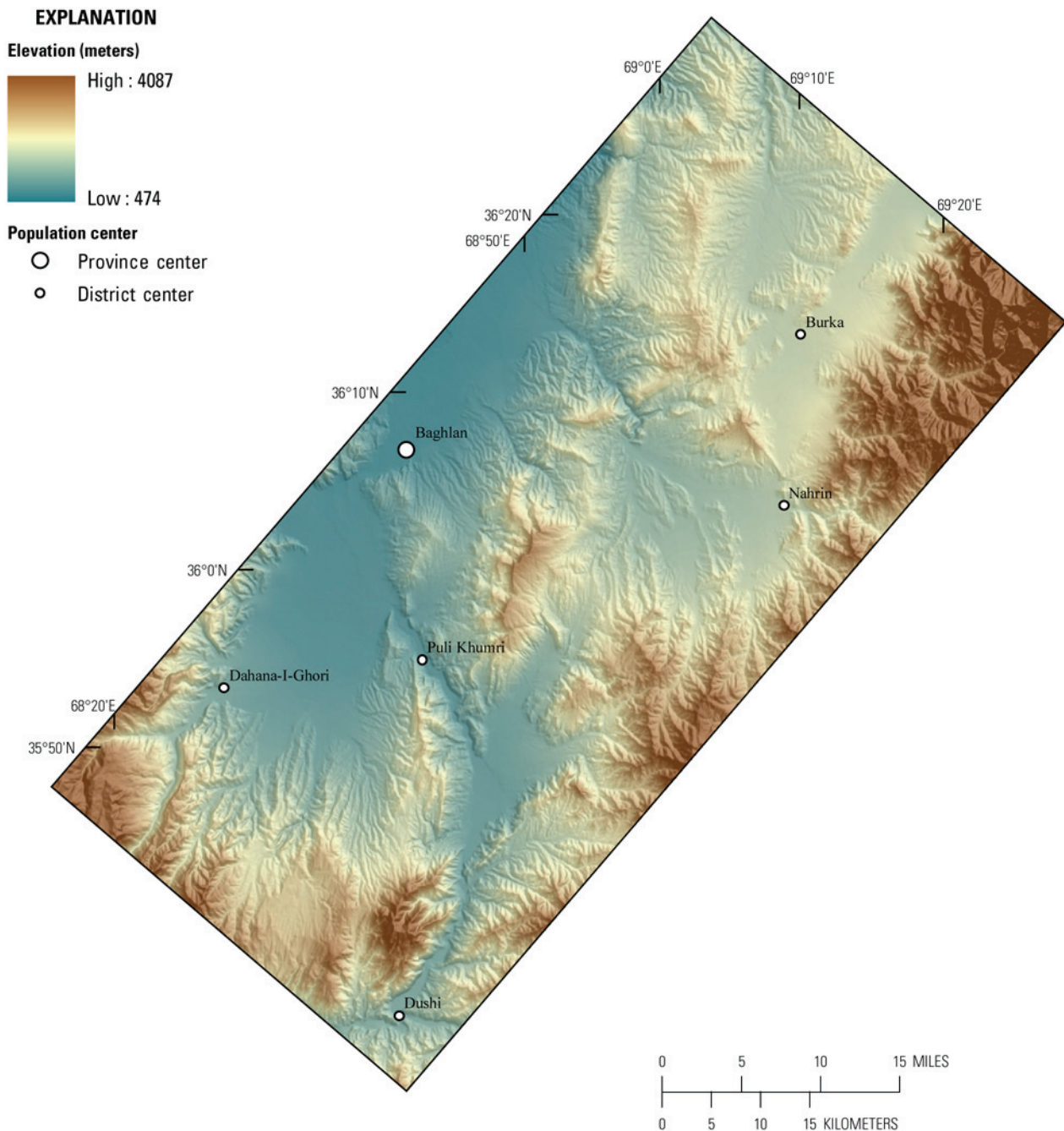


**Figure 19B–3.** Elevations and topography of the Dudkash area of interest.

### 19B.4.3 Iron Oxides and Hydroxides

Conspicuous areas of hematite are found in the center of the Dudkash AOI (fig. 19B–10) in an early Cretaceous unit, the description of which includes red sandstones as rocks that occur within the unit (Abdullah and Chmyriov, 1977; Doebrich and others, 2006). Large concentrations of hematite also appear along the eastern part of the northern edge of the AOI in early Miocene and Eocene units. Goethite and iron hydroxide are more widespread across the AOI compared to hematite. Similar to the 2- $\mu\text{m}$  class of epidote or chlorite, the 1- $\mu\text{m}$  epidote class is found in the southwest part of the AOI.

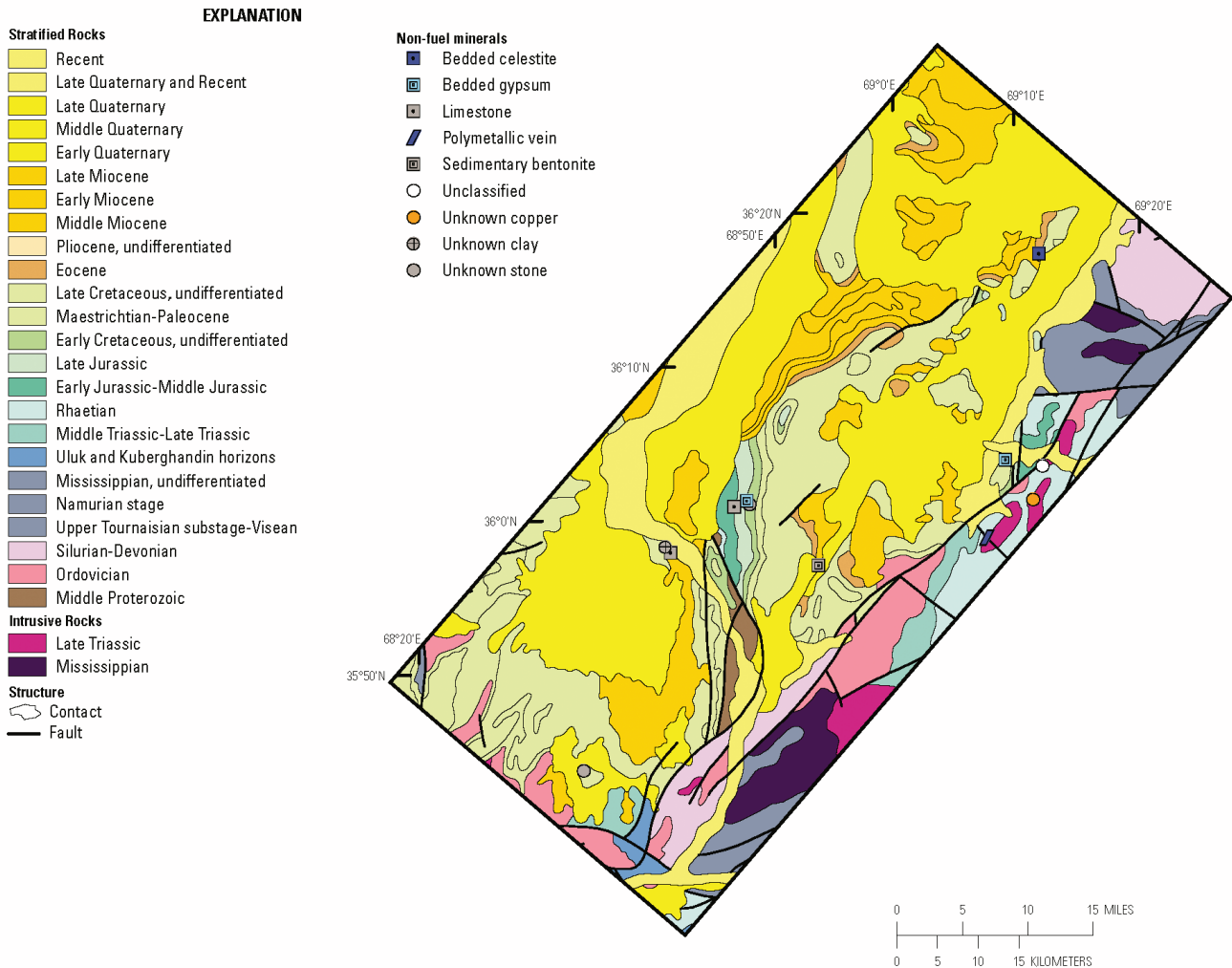


**Figure 19B-4.** Geologic map of the Dudkash area of interest from digital geologic map of Afghanistan (Abdullah and Chmyriov, 1977; Doebrich and others, 2006).

#### 19B.4.4 Common Alteration Minerals

Most of the minerals in this group are commonly present in hydrothermally altered rocks associated with epithermal mineral deposits (fig. 19B-11). Consequently, where they occur in distinct clusters is of great interest in terms of potential mineral deposits. However, the mineral distributions do not occur in distributions that are suggestive of such alteration in the Dudkash AOI.

#### 19B.4.5 Common Secondary Minerals

Secondary minerals, in the epidote and chlorite or epidote classes (fig. 19B-12), occur mostly along the southern edge of the Dudkash AOI, near the town of Dushi. In addition, there are concentrations of pixels matched to the epidote and chlorite or epidote classes in the northeast part of the Dudkash AOI, northeast of the town of Nahrin. In both these areas, epidote and chlorite are mapped within Namurian stage and Mississippian stratified rocks, similar to the distributions of epidote and chlorite pixels in rocks of these ages in the Takhar AOI (Kokaly and Johnson, chap. 26B of this report).

#### 19B.4.6 Gypsum

A MICA analysis using only gypsum in the reference spectral library was conducted to expand the mapping of gypsum for greater detail. However, that resulted in only a few isolated, small concentrations of gypsum being detected in the Dudkash area. A grouping of four pixels containing



Name	Deposit type	Major commodity	Deposit size, description	Alteration	Mineralogy	Gangue
Dudkash stone	Unknown stone	Fluxstone	Small, thickness: 3.9 m	nd	Dolomite	nd
Shuraw	Bedded gypsum	Gypsum	Occurrence, thickness: 1 m	nd	Gypsum	nd
Dudkash gypsum	Bedded gypsum	Gypsum	Occurrence, thickness: 1.5 to 2 m (occasionally up to 6 m), extent: up to 12 km	nd	Gypsum	nd
Dudkash lime	Limestone	Limestone	Small, thickness: 30 m	nd	nd	nd
Pul-i-Khumry	Limestone	Limestone	Small, thickness: 300 to 500 m, area: a few thousand m <sup>2</sup>	nd	nd	nd
Unnamed	Polymetallic vein	Zinc	Showing, thickness: 0.5 m	Quartz alteration; silicification; limonitization	Chalcopyrite; galena; malachite	Quartz
Tangi-Murch	Bedded celestite	Celestite	Small, thickness: 0.4 to 1.67 m, extent: up to 170 m	nd	Celestite	nd

### 19B.4.7 Coal

Direct detection of coal was not attempted using spectral feature analysis of imaging spectrometer data, due to coal's lack of diagnostic absorption features. A comparison of the 2- $\mu$ m map of materials, which includes clays, carbonates, phyllosilicates, sulfates, and altered minerals, to known occurrences of coal (Abdullah and others, 1977) and the Lower to Middle Jurassic geologic unit associated with coal is shown in figure 19B–13. The known coal deposits appear to be associated with areas of kaolinite, kaolinite mixed with muscovite/clay/calcite, and calcite mixed with muscovite/illite. This pattern of minerals detected in the HyMap data within and around the Lower to Middle Jurassic geologic unit is the same pattern observed in the Takhar AOI (Kokaly and Johnson, chap. 26, this volume). Given this indication, further study of these associations and refinement of HyMap analysis using spectral measurements of field samples of surface materials common to the known coal resources is warranted.

### 19B.4.8 Celestite

Celestite was not included as a reference material in the 1- $\mu$ m or 2- $\mu$ m MICA analyses of imaging spectrometer data. An examination of the 2- $\mu$ m map of materials, which includes clays, carbonates, phyllosilicates, sulfates, and altered minerals, to the location of the Tangi-Murch celestite deposit (Abdullah and others, 1977) revealed the site to be surrounded by pixels that mapped as calcite. This is consistent with the deposit description as celestite hosted by bituminous limestone and surrounded by carbonate rocks. As described previously, calcite is the most abundantly mapped mineral in the area and, therefore, additional understanding of the spectral characteristics of the celestite mineral and the deposit need to be developed in order to derive methods to differentiate the deposit from other limestones and calcite-bearing rocks.

## 19B.5 Summary

Carbonate minerals cover most of the Dudkash AOI. Muscovites were detected in greatest concentration in the mapped units of Mississippian and Late Triassic intrusive rocks in the southwest part of the Dudkash AOI and in the adjacent units, suggesting that mineral distributions detected with HyMap data could help in the refinement of lithologic contacts. Epidote and chlorite were found in spatially consistent patterns near the southern edge of the AOI in association with Namurian stage and Mississippian stratified rock units, also suggesting the mineral classes derived from imaging spectrometer data is revealing subdivisions in the mapped unit. Distinct patterns of kaolinite clays and gypsum occur in localized patterns, especially in the center of the AOI. Kaolinites were distributed mostly in Early and Middle Jurassic units, with additional occurrences of spatially consistent groups of pixels in Late Jurassic and Late Cretaceous units. In the center of the Dudkash AOI, kaolinite is found in

association with the Dudkash bedded gypsum mineral deposit. The spectral signature of gypsum was detected in the HyMap data in just a few pixels, some of which were adjacent to the mapped locations of the bedded gypsum mineral occurrence of Shuraw. Within and around rocks of Early to Middle Jurassic age, the known coal deposits appear to be associated with pixels in which kaolinite mixed with other materials was mapped in the HyMap data, an association also observed in the Takhar AOI (Kokaly and Johnson, chap. 26, this volume). Given these indications, more detailed analysis of HyMap data around these coal occurrences may help characterize and refine the distribution of this resource. The limestone host rock of celestite was detected; however, more detailed studies of the spectral characteristics of the celestite deposit and its host rocks are needed in order to characterize the resource and map its distribution using the HyMap imaging spectrometer data covering the Dudkash AOI.

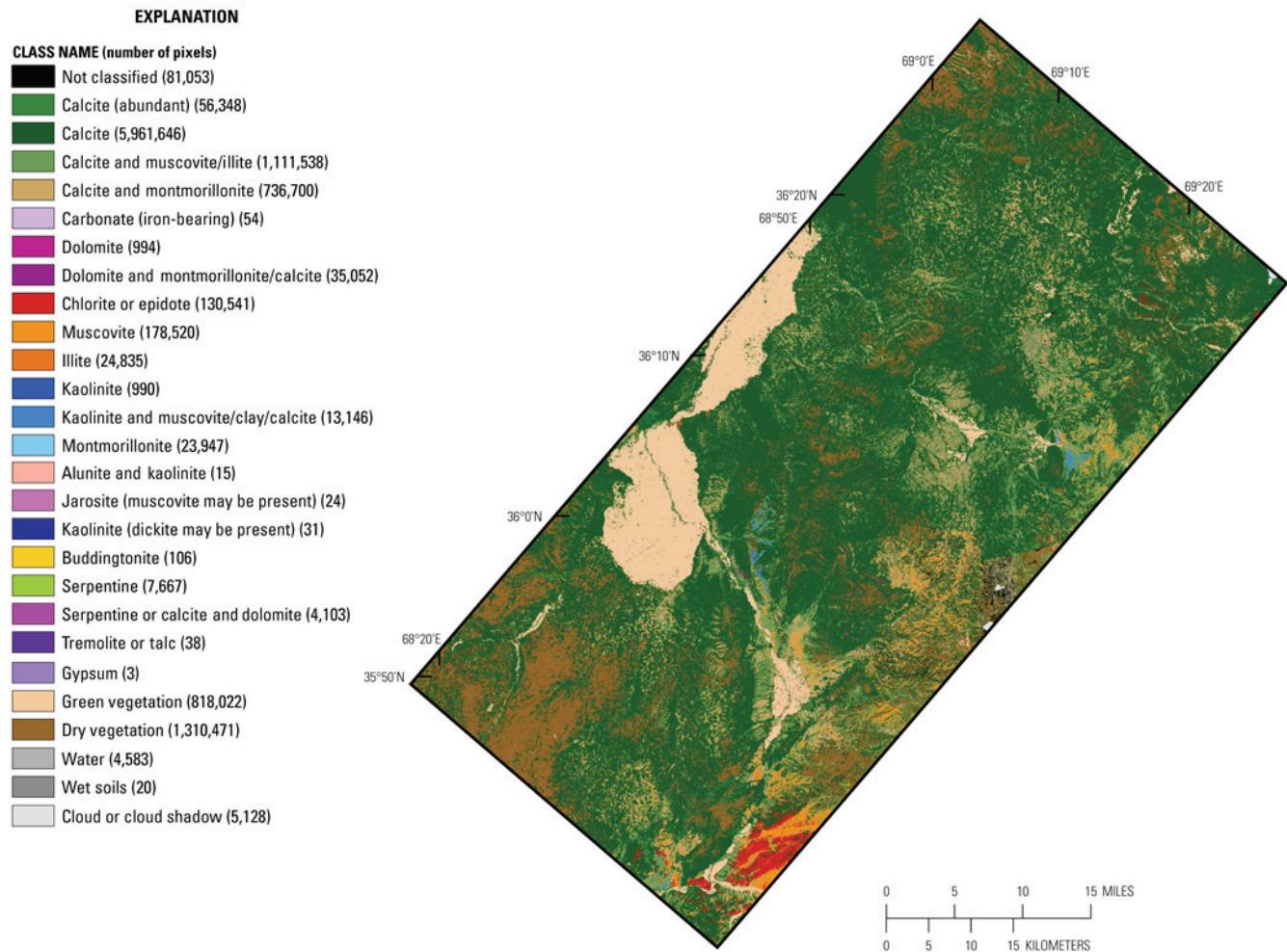


**Figure 19B–6.** Map of carbonates, phyllosilicates, sulfates, altered minerals, and other materials derived from HyMap data in the Dudkash area of interest.

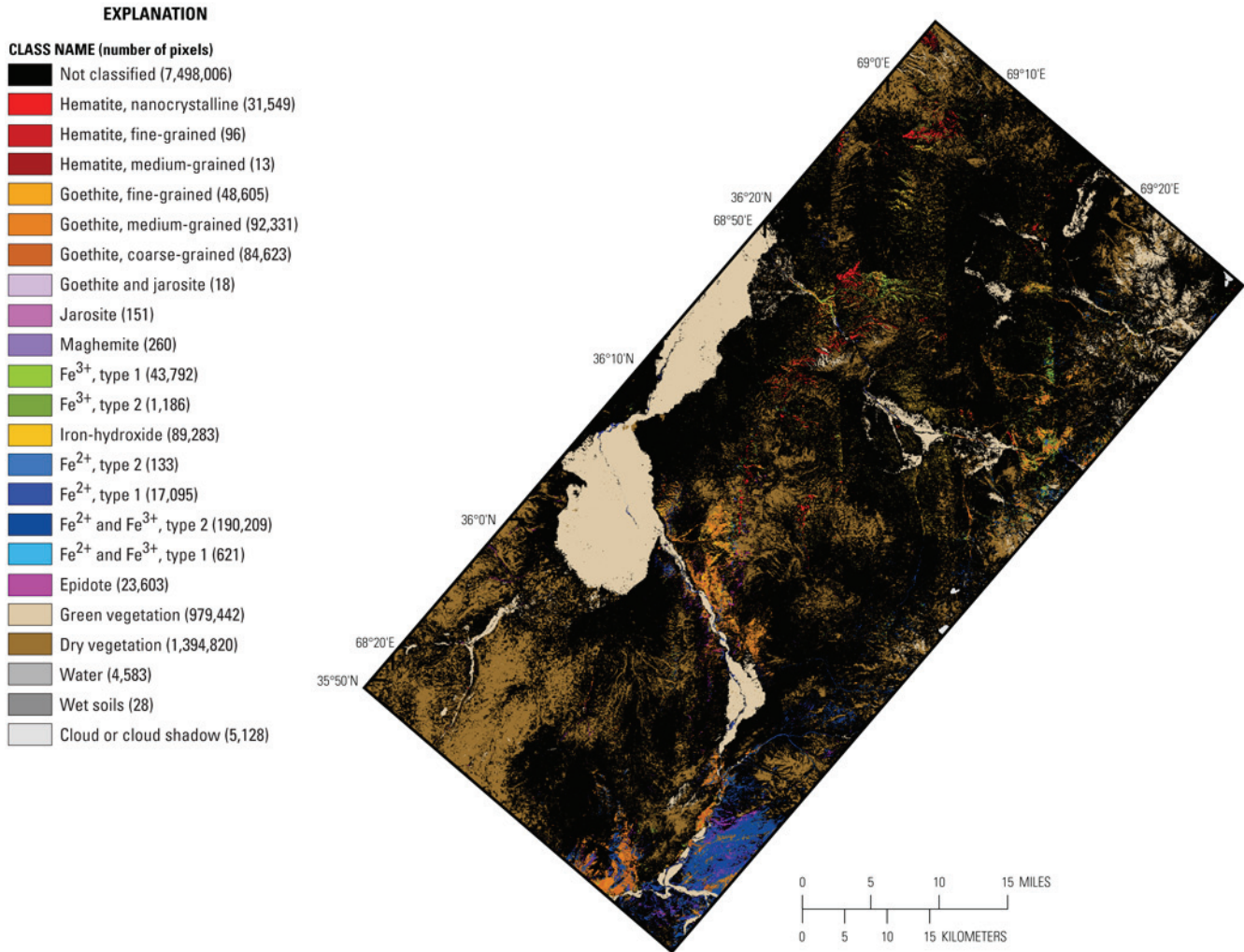


**Figure 19B–7.** Map of iron-bearing minerals and other materials derived from HyMap data in the Dudkash area of interest.

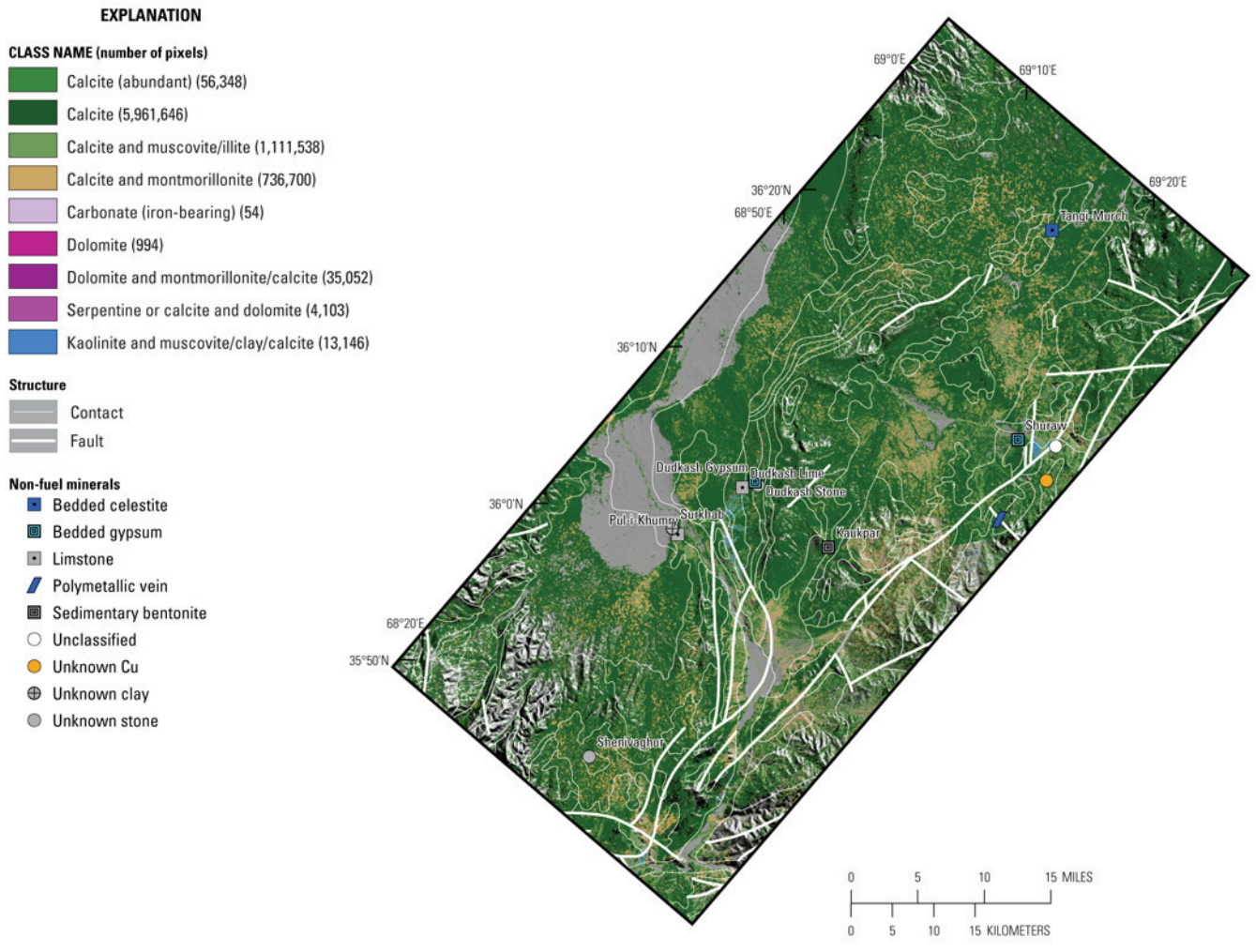


**Figure 19B–8.** Map of distribution of carbonate minerals derived from HyMap data in the Dudkash area of interest.

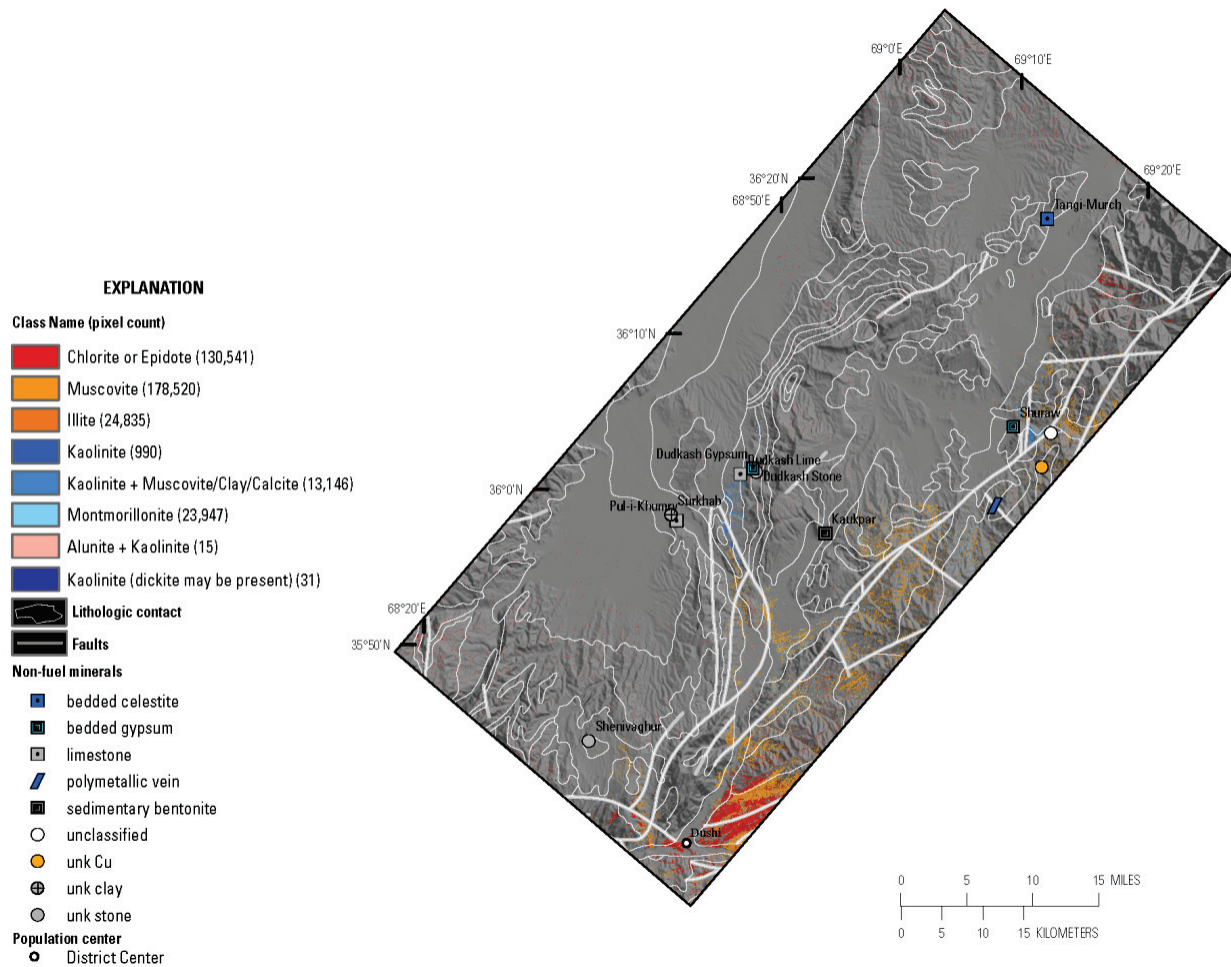


**Figure 19B–9.** Map of distribution of clay and mica minerals derived from HyMap data in the Dudkash area of interest.

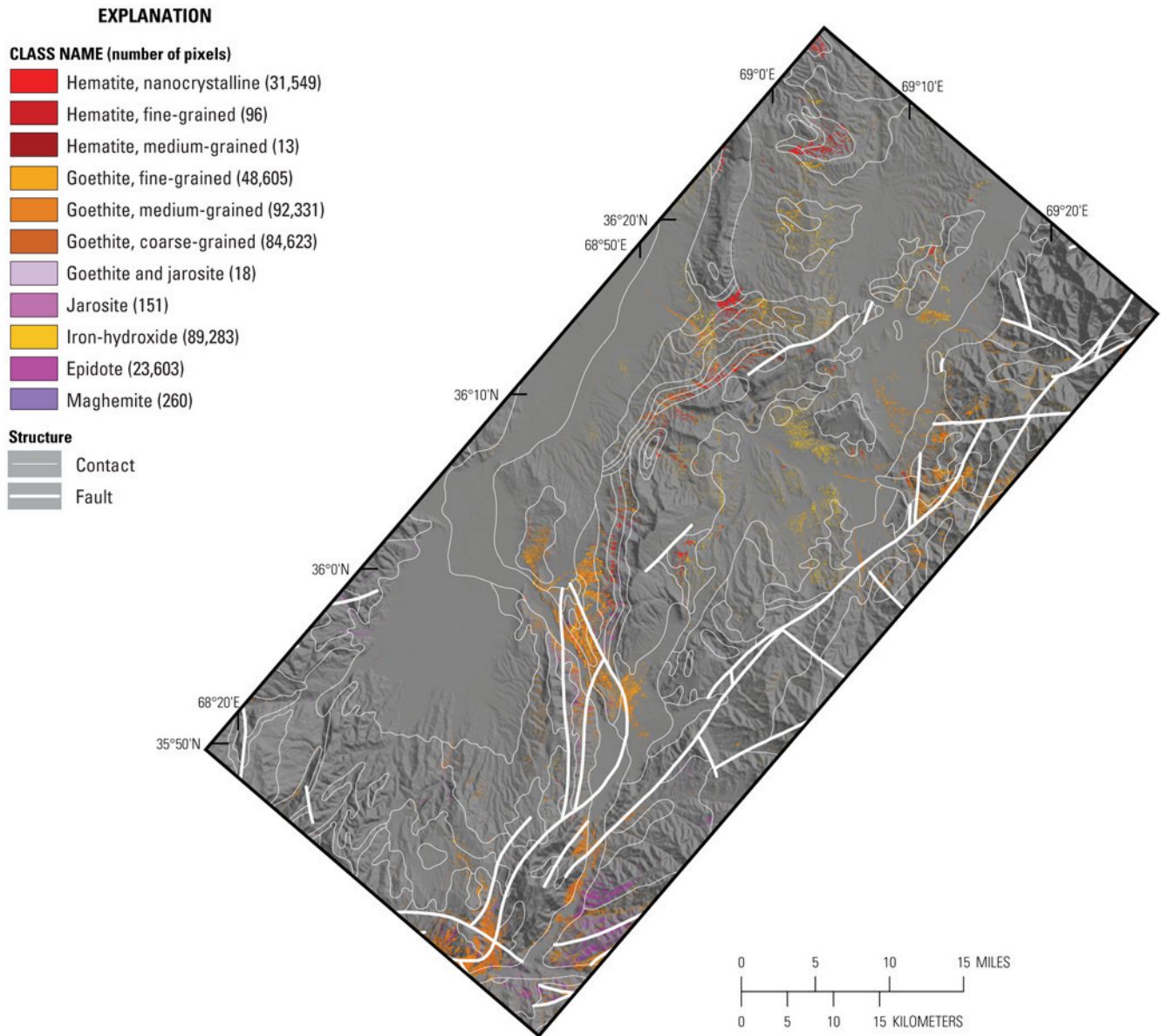


**Figure 19B–10.** Map of distribution of iron oxide and hydroxide derived from HyMap data in the Dudkash area of interest.

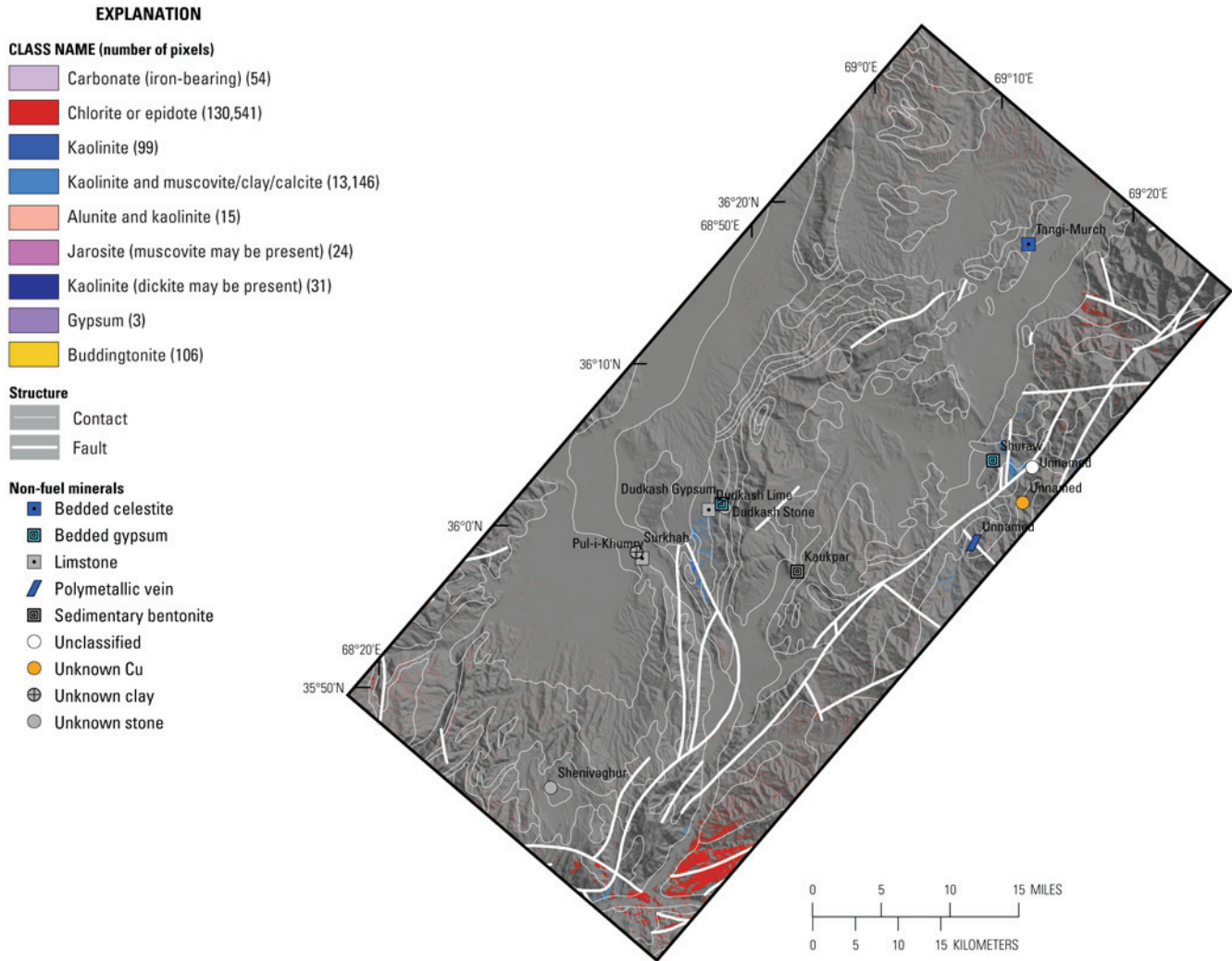


**Figure 19B–11.** Map of distribution of common alteration minerals derived from HyMap data in the Dudkash area of interest.

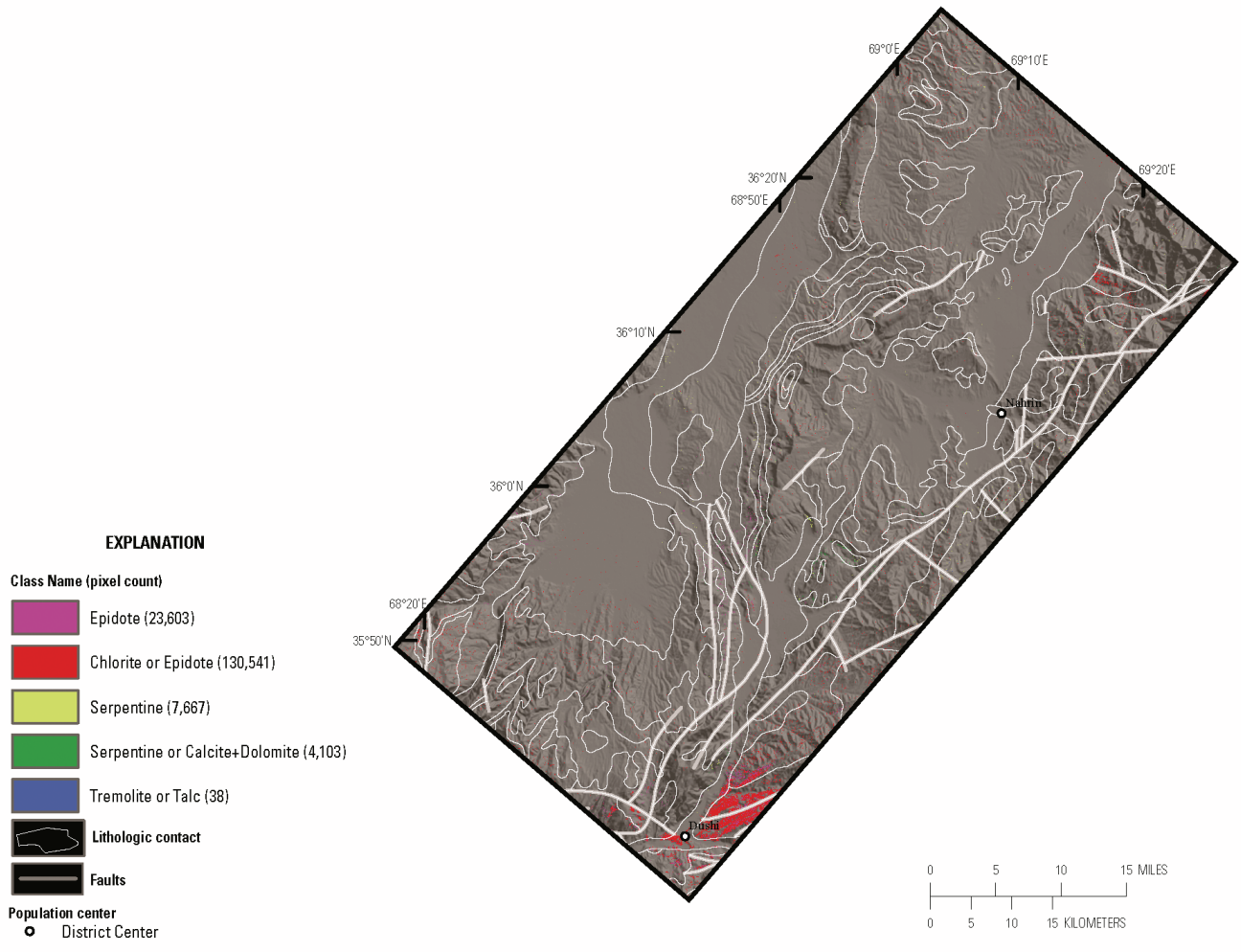


**Figure 19B–12.** Map of distribution of common secondary minerals derived from HyMap data in the Dudkash area of interest.

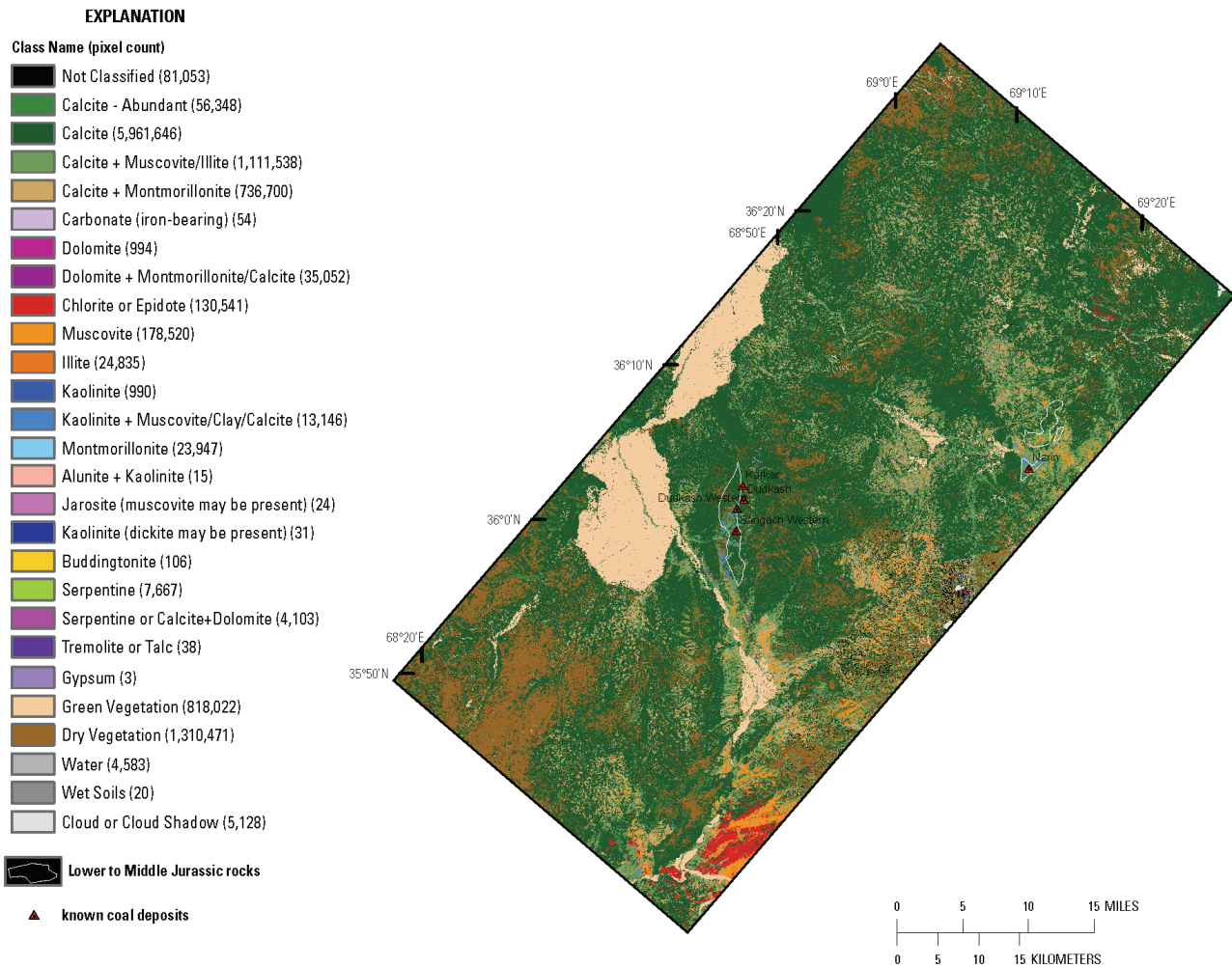


**Figure 19B–13.** Map of carbonates, phyllosilicates, sulfates, altered minerals, and other materials derived from HyMap data in relation to known coal occurrences (Abdullah and others, 1977) in the Dudkash area of interest.

## 19B.6 References Cited

- Abdullah, Sh., and Chmyriov, V.M., 1977, Geological map of Afghanistan: Kabul, Afghanistan, Ministry of Mining and Industry of the Democratic Republic of Afghanistan, scale 1:500,000.
- Abdullah, Sh., Chmyriov, V.M., Stazhilo-Alekseev, K.F., Dronov, V.I., Gannan, P.J., Rossovskiy, L.N., Kafarskiy, A.Kh., and Malyarov, E.P., 1977, Mineral resources of Afghanistan (2d ed.): Kabul, Afghanistan, Republic of Afghanistan Geological and Mineral Survey, 419 p.
- Cocks, T., Jenssen, R., Stewart, A., Wilson, I., and Shields, T., 1998, The HyMap airborne hyperspectral sensor—The system, calibration and performance, *in* Schaepman, M., Schlapfer, D., and Itten, K.I., eds., Proceedings of the 1st EARSel Workshop on Imaging Spectroscopy, 6–8 October 1998, Zurich: Paris, European Association of Remote Sensing Laboratories, p. 37–43.
- Davis, P.A., 2007, Landsat ETM+ false-color image mosaics of Afghanistan: U.S. Geological Survey Open-File Report 2007–1029, 22 p. (Also available at <http://pubs.usgs.gov/of/2007/1029/>.)
- Doeblich, J.L., and Wahl, R.R., comps., *with contributions by* Doeblich, J.L., Wahl, R.R., Ludington, S.D., Chirico, P.G., Wandrey, C.J., Bohannon, R.G., Orris, G.J., Bliss, J.D., and \_\_\_\_\_ 2006, Geologic and mineral resource map of Afghanistan: U.S. Geological Survey Open File Report 2006–1038, scale 1:850,000, available at <http://pubs.usgs.gov/of/2006/1038/>.

- Hoefen, T.M., Kokaly, R.F., and King, T.V.V., 2010, Calibration of HyMap data covering the country of Afghanistan, *in* Proceedings of the 15th Australasian Remote Sensing and Photogrammetry Conference, Alice Springs, Australia, September 12–17, 2010, p. 409, available at <http://dl.dropbox.com/u/81114/15ARSPC-Proceedings.zip/>.
- King, T.V.V., Kokaly, R.F., Hoefen, T.M., and Knepper, D.H., 2010, Resource mapping in Afghanistan using HyMap data, *in* Proceedings of the 15th Australasian Remote Sensing and Photogrammetry Conference, Alice Springs, Australia, September 12–17, 2010, p. 500, available at <http://dl.dropbox.com/u/81114/15ARSPC-Proceedings.zip/>.
- King, T.V.V., Kokaly, R.F., Hoefen, T.M., Dudek, K. and Livo, K.E., 2011, Surface materials map of Afghanistan—Iron-bearing minerals and other materials: U.S. Geological Survey Scientific Investigations Map 3152–B.
- Kokaly, R.F., King, T.V.V., and Livo, K.E., 2008, Airborne hyperspectral survey of Afghanistan 2007: Flight line planning and HyMap data collection: U.S. Geological Survey Open-File Report 2008–1235, 14 p.
- Kokaly, Ray, 2011, PRISM—Processing routines in IDL for spectroscopic measurements: U.S. Geological Survey Open-File Report 2011–1155, available at <http://pubs.usgs.gov/of/2011/1155/>.
- Kokaly, R.F., King, T.V.V., Hoefen, T.M., Dudek, K. and Livo, K.E., 2011, Surface materials map of Afghanistan—Carbonates, phyllosilicates, sulfates, altered minerals, and other materials: U.S. Geological Survey Scientific Investigations Map 3152–A.
- Peters, S.G., Ludington, S.D., Orris, G.J., Sutphin, D.M., Bliss, J.D., and Rytuba, J.J., eds., and the U.S. Geological Survey-Afghanistan Ministry of Mines Joint Mineral Resource Assessment Team, 2007, Preliminary non-fuel mineral resource assessment of Afghanistan: U.S. Geological Survey Open-File Report 2007–1214, 810 p., 1 CD-ROM. (Also available at <http://pubs.usgs.gov/of/2007/1214/>.)